Observation of $e^+e^- \to \eta J/\psi$ at center-of-mass energy $\sqrt{s} = 4.009$ GeV

M. Ablikim,[1] M. N. Achasov,[5] D. J. Ambrose,[39] F. F. An,[1] Q. An,[40] Z. H. An,[1] J. Z. Bai,[1] Y. Ban,[27] J. Becker,[2] J. V. Bennett,[17] M. Bertani,[18a] J. M. Bian,[38] E. Boger,[20,*] O. Bondarenko,[21] I. Boyko,[20] R. A. Briere,[3] V. Bytev,[20] X. Cai,[1] O. Cakir,[35a] A. Calcaterra,[18a] G. F. Cao,[1] S. A. Cetin,[35b] J. F. Chang,[1] G. Chelkov,[20,*] G. Chen,[1] H. S. Chen,[1] J. C. Chen,[1] M. L. Chen,[1] S. J. Chen,[25] Y. B. Chen,[1] H. P. Cheng,[14] Y. P. Chu,[1] D. Cronin-Hennessy,[38] H. L. Dai,[1] J. P. Dai,[1] D. Dedovich,[20] Z. Y. Deng,[1] A. Denig,[19] I. Denysenko,[20,†] M. Destefanis,[43a,43c] W. M. Ding,[29] Y. Ding,[23] L. Y. Dong,[1] M. Y. Dong,[1] S. X. Du,[46] J. Fang,[1] S. S. Fang,[1] L. Fava,[43b,43c] F. Feldbauer,[2] C. Q. Feng,[40] R. B. Ferroli,[18a] C. D. Fu,[1] J. L. Fu,[25] Y. Gao,[34] C. Geng,[40] K. Goetzen,[7] W. X. Gong,[1] W. Gradl,[19] M. Greco,[43a,43c] M. H. Gu,[1] Y. T. Gu,[9] Y. H. Guan,[6] A. Q. Guo,[26] L. B. Guo,[24] Y. P. Guo,[26] Y. L. Han,[1] F. A. Harris,[37] K. L. He,[1] M. He,[1] Z. Y. He,[26] T. Held,[2] Y. K. Heng,[1] Z. L. Hou,[1] H. M. Hu,[1] J. F. Hu,[6] T. Hu,[1] G. M. Huang,[15] J. S. Huang,[12] X. T. Huang,[29] Y. P. Huang,[1] T. Hussain,[42] C. S. Ji,[40] Q. Ji,[1] X. B. Ji,[1] X. L. Ji,[1] L. L. Jiang,[1] X. S. Jiang,[1] J. B. Jiao,[29] Z. Jiao,[14] D. P. Jin,[1] S. Jin,[1] F. F. Jing,[34] N. Kalantar-Nayestanaki,[21] M. Kavatsyuk,[21] W. Kuehn,[36] W. Lai,[1] J. S. Lange,[36] C. H. Li,[1] Cheng Li,[40] Cui Li,[40] D. M. Li,[46] F. Li,[1] G. Li,[1] H. B. Li,[1] J. C. Li,[1] K. Li,[10] Lei Li,[1] Q. J. Li,[1] S. L. Li,[1] W. D. Li,[1] W. G. Li,[1] X. L. Li,[29] X. N. Li,[1] X. Q. Li,[26] X. R. Li,[28] Z. B. Li,[33] H. Liang,[40] Y. F. Liang,[31] Y. T. Liang,[36] G. R. Liao,[34] X. T. Liao,[1] B. J. Liu,[1] C. L. Liu,[3] C. X. Liu,[1] C. Y. Liu,[1] F. H. Liu,[30] Fang Liu,[1] Feng Liu,[15] H. Liu,[1] H. B. Liu,[6] H. H. Liu,[13] H. M. Liu,[1] H. W. Liu,[1] J. P. Liu,[44] K. Y. Liu,[23] Kai Liu,[6] P. L. Liu,[29] Q. Liu,[6] S. B. Liu,[40] X. Liu,[22] X. H. Liu,[1] Y. B. Liu,[26] Z. A. Liu,[1] Zhiqiang Liu,[1] Zhiqing Liu,[1] H. Loehner,[21] G. R. Lu,[12] H. J. Lu,[14] J. G. Lu,[1] Q. W. Lu,[30] X. R. Lu,[6] Y. P. Lu,[1] C. L. Luo,[24] M. X. Luo,[45] T. Luo,[37] X. L. Luo,[1] M. Lv,[1] C. L. Ma,[6] F. C. Ma,[23] H. L. Ma,[1] Q. M. Ma,[1] S. Ma,[1] T. Ma,[1] X. Y. Ma,[1] Y. Ma,[11] F. E. Maas,[11] M. Maggiora,[43a,43c] Q. A. Malik,[42] Y. J. Mao,[27] Z. P. Mao,[1] J. G. Messchendorp,[21] J. Min,[1] T. J. Min,[1] R. E. Mitchell,[17] X. H. Mo,[1] C. Morales Morales,[11] C. Motzko,[2] N. Yu. Muchnoi,[5] H. Muramatsu,[39] Y. Nefedov,[20] C. Nicholson,[6] I. B. Nikolaev,[5] Z. Ning,[1] S. L. Olsen,[28] Q. Ouyang,[1] S. Pacetti,[18b] J. W. Park,[28] M. Pelizaeus,[37] H. P. Peng,[40] K. Peters,[7] J. L. Ping,[24] R. G. Ping,[1] R. Poling,[38] E. Prencipe,[19] M. Qi,[25] S. Qian,[1] C. F. Qiao,[6] X. S. Qin,[1] Y. Qin,[27] Z. H. Qin,[1] J. F. Qiu,[1] K. H. Rashid,[42] G. Rong,[1] X. D. Ruan,[9] A. Sarantsev,[20,‡] B. D. Schaefer,[17] J. Schulze,[2] M. Shao,[40] C. P. Shen,[37,§] X. Y. Shen,[1] H. Y. Sheng,[1] M. R. Shepherd,[17] W. M. Song,[1] X. Y. Song,[1] S. Spataro,[43a,43c] B. Spruck,[36] D. H. Sun,[1] G. X. Sun,[1] J. F. Sun,[12] S. S. Sun,[1] Y. J. Sun,[40] Y. Z. Sun,[1] Z. J. Sun,[1] Z. T. Sun,[40] C. J. Tang,[31] X. Tang,[1] I. Tapan,[35c] E. H. Thorndike,[39] D. Toth,[38] M. Ullrich,[36] G. S. Varner,[37] B. Wang,[9] B. Q. Wang,[27] K. Wang,[1] L. L. Wang,[4] L. S. Wang,[1] M. Wang,[29] P. Wang,[1] P. L. Wang,[1] Q. Wang,[1] Q. J. Wang,[1] S. G. Wang,[27] X. L. Wang,[40] Y. D. Wang,[40] Y. F. Wang,[1] Y. Q. Wang,[29] Z. Wang,[1] Z. G. Wang,[1] Z. Y. Wang,[1] D. H. Wei,[8] P. Weidenkaff,[19] Q. G. Wen,[40] S. P. Wen,[1] M. Werner,[36] U. Wiedner,[2] L. H. Wu,[1] N. Wu,[1] S. X. Wu,[40] W. Wu,[26] Z. Wu,[1] L. G. Xia,[34] Z. J. Xiao,[24] Y. G. Xie,[1] Q. L. Xiu,[1] G. F. Xu,[1] G. M. Xu,[27] H. Xu,[1] Q. J. Xu,[10] X. P. Xu,[32] Z. R. Xu,[40] F. Xue,[15] Z. Xue,[1] L. Yan,[40] W. B. Yan,[40] Y. H. Yan,[16] H. X. Yang,[1] Y. Yang,[15] Y. X. Yang,[8] H. Ye,[1] M. Ye,[1] M. H. Ye,[4] B. X. Yu,[1] C. X. Yu,[26] J. S. Yu,[22] S. P. Yu,[29] C. Z. Yuan,[1] Y. Yuan,[1] A. A. Zafar,[42] A. Zallo,[18a] Y. Zeng,[16] B. X. Zhang,[1] B. Y. Zhang,[1] C. C. Zhang,[1] D. H. Zhang,[1] H. H. Zhang,[33] H. Y. Zhang,[1] J. Q. Zhang,[1] J. W. Zhang,[1] J. Y. Zhang,[1] J. Z. Zhang,[1] S. H. Zhang,[1] X. J. Zhang,[1] X. Y. Zhang,[29] Y. Zhang,[1] Y. H. Zhang,[1] Y. S. Zhang,[9] Z. P. Zhang,[40] Z. Y. Zhang,[44] G. Zhao,[1] H. S. Zhao,[1] J. W. Zhao,[1] K. X. Zhao,[24] Lei Zhao,[40] Ling Zhao,[1] M. G. Zhao,[26] Q. Zhao,[1] S. J. Zhao,[46] T. C. Zhao,[1] X. H. Zhao,[25] Y. B. Zhao,[1] Z. G. Zhao,[40] A. Zhemchugov,[20,*] B. Zheng,[41] J. P. Zheng,[1] Y. H. Zheng,[6] B. Zhong,[1] J. Zhong,[2] L. Zhou,[1] X. K. Zhou,[6] X. R. Zhou,[40] C. Zhu,[1] K. Zhu,[1] K. J. Zhu,[1] S. H. Zhu,[1] X. L. Zhu,[34] X. W. Zhu,[1] Y. C. Zhu,[40] Y. M. Zhu,[26] Y. S. Zhu,[1] Z. A. Zhu,[1] J. Zhuang,[1] B. S. Zou,[1] and J. H. Zou,[1]

(BESIII Collaboration)

[1]*Institute of High Energy Physics, Beijing 100049, People's Republic of China*
[2]*Bochum Ruhr-University, 44780 Bochum, Germany*
[3]*Carnegie Mellon University, Pittsburgh, Pennsylvania 15213, USA*
[4]*China Center of Advanced Science and Technology, Beijing 100190, People's Republic of China*
[5]*G. I. Budker Institute of Nuclear Physics SB RAS (BINP), Novosibirsk 630090, Russia*
[6]*Graduate University of Chinese Academy of Sciences, Beijing 100049, People's Republic of China*
[7]*GSI Helmholtzcentre for Heavy Ion Research GmbH, D-64291 Darmstadt, Germany*
[8]*Guangxi Normal University, Guilin 541004, People's Republic of China*
[9]*GuangXi University, Nanning 530004, People's Republic of China*
[10]*Hangzhou Normal University, Hangzhou 310036, People's Republic of China*
[11]*Helmholtz Institute Mainz, J. J. Becherweg 45,D 55099 Mainz, Germany*

[12]*Henan Normal University, Xinxiang 453007, People's Republic of China*

[13]*Henan University of Science and Technology, Luoyang 471003, People's Republic of China*

[14]*Huangshan College, Huangshan 245000, People's Republic of China*

[15]*Huazhong Normal University, Wuhan 430079, People's Republic of China*

[16]*Hunan University, Changsha 410082, People's Republic of China*

[17]*Indiana University, Bloomington, Indiana 47405, USA*

[18a]*INFN Laboratori Nazionali di Frascati, Frascati, Italy*

[18b]*INFN and University of Perugia, I-06100, Perugia, Italy*

[19]*Johannes Gutenberg University of Mainz, Johann-Joachim-Becher-Weg 45, 55099 Mainz, Germany*

[20]*Joint Institute for Nuclear Research, 141980 Dubna, Russia*

[21]*KVI/University of Groningen, 9747 AA Groningen, Netherlands*

[22]*Lanzhou University, Lanzhou 730000, People's Republic of China*

[23]*Liaoning University, Shenyang 110036, People's Republic of China*

[24]*Nanjing Normal University, Nanjing 210046, People's Republic of China*

[25]*Nanjing University, Nanjing 210093, People's Republic of China*

[26]*Nankai University, Tianjin 300071, People's Republic of China*

[27]*Peking University, Beijing 100871, People's Republic of China*

[28]*Seoul National University, Seoul, 151-747 Korea*

[29]*Shandong University, Jinan 250100, People's Republic of China*

[30]*Shanxi University, Taiyuan 030006, People's Republic of China*

[31]*Sichuan University, Chengdu 610064, People's Republic of China*

[32]*Soochow University, Suzhou 215006, People's Republic of China*

[33]*Sun Yat-Sen University, Guangzhou 510275, People's Republic of China*

[34]*Tsinghua University, Beijing 100084, People's Republic of China*

[35a]*Ankara University, Ankara, Turkey*

[35b]*Dogus University, Istanbul, Turkey*

[35c]*Uludag University, Bursa, Turkey*

[36]*Universitaet Giessen, 35392 Giessen, Germany*

[37]*University of Hawaii, Honolulu, Hawaii 96822, USA*

[38]*University of Minnesota, Minneapolis, Minnesota 55455, USA*

[39]*University of Rochester, Rochester, New York 14627, USA*

[40]*University of Science and Technology of China, Hefei 230026, People's Republic of China*

[41]*University of South China, Hengyang 421001, People's Republic of China*

[42]*University of the Punjab, Lahore-54590, Pakistan*

[43a]*University of Turin, Turin, Italy*

[43b]*University of Eastern Piedmont, Alessandria, Italy*

[43c]*INFN, Turin, Italy*

[44]*Wuhan University, Wuhan 430072, People's Republic of China*

[45]*Zhejiang University, Hangzhou 310027, People's Republic of China*

[46]*Zhengzhou University, Zhengzhou 450001, People's Republic of China*

Using a 478 pb^{-1} data sample collected with the BESIII detector operating at the Beijing Electron Positron Collider storage ring at a center-of-mass energy of $\sqrt{s} = 4.009$ GeV, the production of $e^+ e^- \rightarrow \eta J/\psi$ is observed for the first time with a statistical significance of greater than 10σ. The Born cross section is measured to be $(32.1 \pm 2.8 \pm 1.3)$ pb, where the first error is statistical and the second systematic. Assuming the $\eta J/\psi$ signal is from a hadronic transition of the $\psi(4040)$, the fractional transition rate is determined to be $\mathcal{B}(\psi(4040) \rightarrow \eta J/\psi) = (5.2 \pm 0.5 \pm 0.2 \pm 0.5) \times 10^{-3}$, where the first, second, and third errors are statistical, systematic, and the uncertainty from the $\psi(4040)$ resonant parameters, respectively. The production of $e^+ e^- \rightarrow \pi^0 J/\psi$ is searched for, but no significant signal is observed, and $\mathcal{B}(\psi(4040) \rightarrow \pi^0 J/\psi) < 2.8 \times 10^{-4}$ is obtained at the 90% confidence level.

---

*Also at the Moscow Institute of Physics and Technology, Moscow, Russia.

†On leave from the Bogolyubov Institute for Theoretical Physics, Kiev, Ukraine.

‡Also at the PNPI, Gatchina, Russia.

§Present address: Nagoya University, Nagoya, Japan.

The properties of excited $J^{PC} = 1^{--}$ charmonium states above the $D\bar{D}$ production threshold are of great interest but not well understood, even decades after their first observation [1]. The current experimentally well established structures in the hadronic cross section are the $\psi(3770)$, $\psi(4040)$, $\psi(4160)$, and $\psi(4415)$ resonances [2].

Unlike the low-lying vector $c\bar{c}$ states J/ψ and $\psi(3686)$, all of these states couple to open-charm final states with large partial widths and disfavor hidden-charm decays.

Recently, new vector charmoniumlike states, the $Y(4260)$, the $Y(4360)$ and the $Y(4660)$, have been discovered via their decays into exclusive $\pi^+\pi^-J/\psi$ and $\pi^+\pi^-\psi(3686)$ final states [3]. The common properties of these states are relatively narrow widths and strong couplings to hidden-charm final states. These Y states cannot be assigned to any of the conventional $c\bar{c}$ 1^{--} ψ family states [4] in any natural way and suggest the existence of a nonconventional meson spectroscopy [5].

Hadronic transitions play an important role in understanding the nature of conventional heavy quarkonium. An excess of η over $\pi^+\pi^-$ hidden-bottom transition rates of the $\Upsilon(4S)$ [6] has been explained as an admixture of a four-quark state in the $\Upsilon(4S)$ wave function [7]. A similar picture might be expected in the charm sector but, as of yet, there are no experimental data available for η transitions in the high-mass charmonium and charmoniumlike states, except for evidence of $\psi(3770) \rightarrow \eta J/\psi(3.5\sigma)$ [8] and $\psi(4160) \rightarrow \eta J/\psi(4.0\sigma)$ [9]. Moreover, there are predictions of many new states in various models trying to explain the conventional and unconventional states observed in this mass region [5].

In this Letter, we report cross section measurements for $e^+e^- \rightarrow \eta J/\psi$ and $\pi^0 J/\psi$ at the center-of-mass energy $\sqrt{s} = (4.009 \pm 0.001)$ GeV. The analysis is performed with a 478 pb^{-1} data sample collected with the BESIII detector located at the Beijing Electron Positron Collider storage ring [10]. The integrated luminosity of this data sample was measured using Bhabha events, with an estimated uncertainty of 1.1%. In order to control systematic errors, an accompanying data sample of about 7×10^6 $\psi(3686)$ events was accumulated under the same experimental conditions. In the analysis, the J/ψ is reconstructed through its decays into lepton pairs (e^+e^- and $\mu^+\mu^-$) while η/π^0 is reconstructed in the $\gamma\gamma$ final state.

The GEANT4-based Monte Carlo (MC) simulation software, which includes the geometric description and the detector response, is used to optimize the event selection criteria, determine the detection efficiency, and estimate the backgrounds. Signal $e^+e^- \rightarrow \eta J/\psi$ and $\pi^0 J/\psi$ MC samples containing 20 000 events for each channel are generated. Initial state radiation (ISR) is simulated with KKMC [11], assuming $\eta J/\psi$ and $\pi^0 J/\psi$ are produced via $\psi(4040)$ decays, and the $\psi(4040)$ is described by a Breit-Wigner function with a constant width. The maximum energies of the ISR photons are 347 and 700 MeV, corresponding to $\eta J/\psi$ and $\pi^0 J/\psi$ production thresholds, respectively. For backgrounds studies, MC samples equivalent to 1 fb^{-1} integrated luminosity are generated: inclusive $\psi(4040)$ decays, ISR production of low-mass vector charmonium states, and QED events. The known decay modes of the charmonium states are generated with

EVTGEN [12] with branching fractions set to their world average values [2] and the remaining events are generated with LUNDCHARM [13] or PYTHIA [14].

Charged tracks are reconstructed in the main drift chamber, and the number of good charged tracks is required to be two with zero net charge. For each track, the polar angle must satisfy $|\cos\theta| < 0.93$, and the point of closest approach to the e^+e^- interaction point must be within ± 10 cm in the beam direction and within ± 1 cm in the plane perpendicular to the beam direction. A charged track with deposited energy in the electromagnetic calorimeter less than 0.4 GeV is identified as a μ candidate while that with a deposited energy over momentum (E/p) ratio larger than 0.8 is identified as an electron candidate. Both of the charged tracks are required to be either identified as muons or as electrons.

Showers identified as photon candidates must satisfy fiducial and shower-quality requirements. The minimum energy is 25 MeV for electromagnetic calorimeter barrel showers ($|\cos\theta| < 0.8$) and 50 MeV for end-cap showers ($0.86 < |\cos\theta| < 0.92$). To eliminate showers produced by charged particles, a photon must be separated by at least $20°$ from any charged track. Final-state radiation and bremsstrahlung energy loss of leptons are corrected by adding the momentum of photons detected within a $5°$ cone around the lepton momentum direction. The number of good photon candidates is required to be two (the efficiency is over 95%), and the recoil mass of the two photons $M_{\text{recoil}}(\gamma\gamma) = \sqrt{(P_{\text{CM}} - P1 - P2)^2} \in [2.9, 3.4]$ GeV/c^2 is required to select good J/ψ candidates. Here P_{CM} is the four-momentum of the initial states, and $P1$ and $P2$ are the four-momenta of the two photons.

The lepton pair and the two photons are subject to a four-constraint (4C) kinematic fit to improve the momentum resolution and reduce the background. The chi-square (χ^2) of the kinematic fit is required to be less than 40. In order to reject radiative Bhabha and radiative dimuon ($\gamma e^+e^-/\gamma\mu^+\mu^-$) backgrounds associated with an energetic radiative photon (γ_H) and a low energy fake photon, the invariant mass $M(\gamma_H\ell^+\ell^-)$ is determined from a three-constraint (3C) kinematic fit in which the energy of the low energy photon is allowed to float. Since the fake photon does not contribute in the 3C fit, the $M(\gamma_H\ell^+\ell^-)$ mass distribution is not distorted by the photon energy threshold cutoff, and backgrounds are clearly separated from signal. The requirement $M(\gamma_H\ell^+\ell^-) < 3.93$ GeV/c^2 removes over 50% of radiative Bhabha and radiative dimuon background events with an efficiency greater than 99% for $\eta J/\psi$ and 89% for $\pi^0 J/\psi$.

After imposing all of these selection criteria, the invariant mass distribution of lepton pairs is shown in Fig. 1. A clear J/ψ signal is observed in the $\mu^+\mu^-$ mode while indications of a peak around 3.1 GeV/c^2 also exist in the e^+e^- mode. The remaining dominant backgrounds are surviving radiative dimuon events in $\mu^+\mu^-$ and radiative
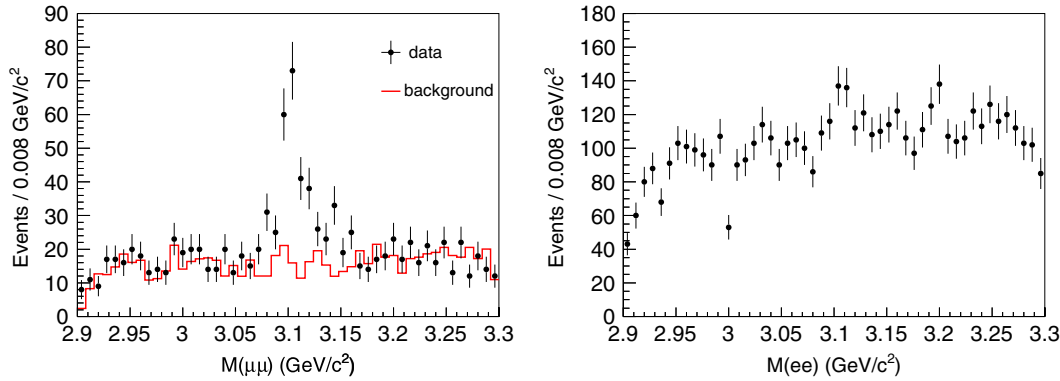
FIG. 1 (color online). (Left panel) $M(\mu^+\mu^-)$ and (right panel) $M(e^+e^-)$ invariant mass distributions. Dots with error bars are data and the open histogram in the left panel shows inclusive-MC-estimated background events.

Bhabha events in e^+e^-; these contribute flat components in the $M(\ell^+\ell^-)$ distributions with no associated peaks in the $M(\gamma\gamma)$ invariant mass distribution. The high background level in the e^+e^- mode is due to the huge background from the Bhabha process. Other possible background sources include $e^+e^- \to \pi^0\pi^0 J/\psi$, $\pi^+\pi^-\pi^0/\pi^+\pi^-\eta$, and $\gamma\chi_{cJ}(1P)/\gamma\chi_{cJ}(2P)$. The $\pi^0\pi^0 J/\psi$ background is estimated by MC simulation to be at the 4.5 pb level and, thus, negligibly small [9]. Potential $\gamma\chi_{cJ}(1P)$ and $\gamma\chi_{cJ}(2P)$ radiative transition backgrounds are estimated using the selected data sample; no significant signal is found for either $\chi_{cJ}(1P)$ or $\chi_{cJ}(2P)$ in $M(\gamma J/\psi)$ mass distribution. The $\pi^+\pi^-\pi^0$ and $\pi^+\pi^-\eta$ backgrounds are estimated using J/ψ sideband events. The ISR-produced vector charmonium backgrounds, including $\gamma_{ISR}J/\psi$, $\gamma_{ISR}\psi(3686)$ and $\gamma_{ISR}\psi(3770)$, are estimated by means of an inclusive MC sample and only 3.3 events in the $\mu^+\mu^-$ mode and 3.1 events in the e^+e^- mode are found (normalized to data luminosity). As they would peak at neither the η nor the π^0 signal region, they are neglected in the analysis.

The resolution of the invariant mass of the lepton pairs is determined to be 14 MeV/c^2 by MC simulation and is in good agreement with events in the $\psi(3686)$ data sample. The mass window of the J/ψ signal is defined as 3.075 GeV/$c^2 < M(\ell^+\ell^-) < 3.125$ GeV/c^2, and the sidebands are defined as 2.95 GeV/$c^2 < M(\ell^+\ell^-) < 3.05$ GeV/c^2 or 3.15 GeV/$c^2 < M(\ell^+\ell^-) < 3.25$ GeV/c^2, which is 4 times as wide as the signal region. Figure 2 shows the $M(\gamma\gamma)$ invariant mass distributions for events in the $J/\psi \to \mu^+\mu^-$ and $J/\psi \to e^+e^-$ signal regions. A significant η signal is observed in both modes. In the $M(\gamma\gamma)$ distribution for J/ψ mass-sideband events, there are backgrounds that peak in the π^0 signal region in $J/\psi \to \mu^+\mu^-$ that originate from $e^+e^- \to \pi^+\pi^-\pi^0$. In order to suppress $e^+e^- \to \pi^+\pi^-\pi^0$ backgrounds, at least one charged track is required to have a muon counter hit a depth larger than 30 cm for the $\pi^0 J/\psi$ signal search. The efficiency for this requirement is 87.9% for signal while about 74% $e^+e^- \to \pi^+\pi^-\pi^0$ background events are rejected. Figure 3 shows the $M(\gamma\gamma)$ invariant mass distribution below 0.3 GeV/c^2 for $J/\psi \to \mu^+\mu^-$.

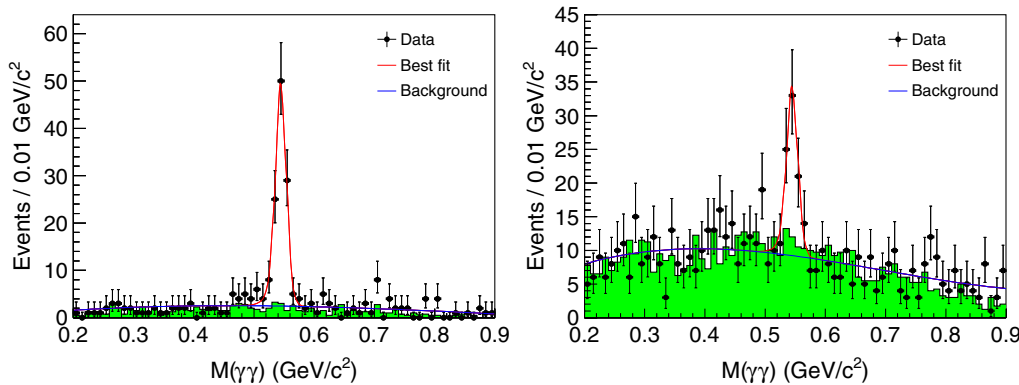FIG. 2 (color online). Distributions of $M(\gamma\gamma)$ between 0.2 and 0.9 GeV/c^2 for $J/\psi \to \mu^+\mu^-$ (left panel) and for $J/\psi \to e^+e^-$ (right panel). Dots with error bars are data in the J/ψ mass signal region, and the green shaded histograms are from normalized J/ψ mass sidebands. The curves show the total fit and the background term.

No significant π^0 signal is observed. We do not analyze $\pi^0 J/\psi$ production in $J/\psi \to e^+e^-$ due to the huge background from Bhabha events. The final selection efficiencies are 38.0% in $\mu^+\mu^-$ and 26.9% in e^+e^- for $\eta J/\psi$, and 31.1% in $\mu^+\mu^-$ for $\pi^0 J/\psi$, according to MC simulation.

The $M(\gamma\gamma)$ invariant mass distributions are fitted using an unbinned maximum likelihood method for $M(\gamma\gamma) < 0.9$ GeV/c^2 in both modes. The probability density function (pdf) for the η/π^0 signal in $J/\psi \to \mu^+\mu^-$ is taken from MC simulation, while in $J/\psi \to e^+e^-$, only the η pdf from MC simulation is used. To account for resolution differences between data and the MC simulation, three Gaussian functions are convolved with the η and the π^0 signal pdfs. For the η signal, the standard deviation of these Gaussians are free while for the π^0 signal it is fixed to (2.4 ± 0.9) MeV/c^2, which is determined from a $\psi(3686) \to \pi^0 J/\psi$ control sample. Background shapes are described by a third-order polynomial. Figure 2 shows the fit results for the η signal and the background contributions for $J/\psi \to \mu^+\mu^-$ and $J/\psi \to e^+e^-$. The fits yield $N^{\rm fit}_{\mu^+\mu^-}(\eta) = 111.4 \pm 11.0$, and $N^{\rm fit}_{e^+e^-}(\eta) = 61.4 \pm 10.5$. The standard deviation of the smearing Gaussian convolved with the η signal is (3.7 ± 1.0) MeV/c^2 in $\mu^+\mu^-$ and (3.7 ± 1.9) MeV/c^2 in e^+e^-. Good agreement is observed between the two modes, and these values are consistent with values from the $\psi(3686) \to \eta J/\psi$ control sample $(3.4 \pm 0.6$ MeV/c^2 in $\mu^+\mu^-$ and 4.6 ± 0.6 MeV/c^2 in $e^+e^-)$. The goodness of fit is estimated by using a χ^2 test method with the data distributions regrouped to ensure that each bin contains more than 10 events. The test gives $\chi^2/\text{ndf} = 14.1/14 = 1.1$ for $\mu^+\mu^-$ and $\chi^2/\text{ndf} = 42.9/43 = 1.0$ for e^+e^-. Figure 3 shows the fit result for the π^0 signal and the background contribution for $J/\psi \to \mu^+\mu^-$. Since the π^0 signal is not

FIG. 3 (color online). Distribution of $M(\gamma\gamma)$ below 0.3 GeV/c^2 for $J/\psi \to \mu^+\mu^-$. Dots with error bars are data in the J/ψ mass signal region, and the green shaded histogram is from normalized J/ψ mass sideband. The curves show the total fit and the background term.

significant, we determine an upper limit for the π^0 signal yield of $N^{\rm up}(\pi^0) < 11.7$ at the 90% confidence level. The $e^+e^- \to \pi^+\pi^-\pi^0$ backgrounds are estimated by fitting the $M(\gamma\gamma)$ distribution of the J/ψ mass-sideband events. The signal pdf for the π^0 is a Gaussian function and that for the background is a third-order polynomial. The fit yields $N^{\rm bkg}_{\mu^+\mu^-}(\pi^0) = 2.8 \pm 1.1$ after normalization. The statistical significances of the η and π^0 signals are examined by means of the difference in log-likelihood value with or without signal in the fit and the change of the number of degrees of freedom (Δndf). For the η signal, the statistical significance is larger than 10σ while that for the π^0 signal is only 1.1σ.

The Born-order cross section is determined from the relation

$$\sigma^B = \frac{N^{\rm fit} - N^{\rm bkg}}{\mathcal{L}_{\rm int}(1 + \delta)\epsilon\mathcal{B}}, \tag{1}$$

where $N^{\rm fit}$ and $N^{\rm bkg}$ are the number of signal events from the fit and the number of background events, respectively; $\mathcal{L}_{\rm int}$ is integrated luminosity; ϵ is selection efficiency; $\mathcal{B}$ is the branching fraction of intermediate states decay; and $(1 + \delta)$ is the radiative correction factor, which is 0.757 according to QED calculation [15].

For the $e^+e^- \to \eta J/\psi$ cross section, we obtain $\sigma^B = 34.8 \pm 3.5$ pb for the $\mu^+\mu^-$ mode, and $\sigma^B = 27.1 \pm 4.7$ pb for the e^+e^- mode. Since the results from the two modes agree with each other, we quote a combined cross section result:

$$\sigma^B(e^+e^- \to \eta J/\psi) = 32.1 \pm 2.8 \text{ pb.} \tag{2}$$

Here the errors are statistical only.

Systematic errors mainly come from the luminosity measurement, detection efficiency, background estimation and branching fractions of intermediate states decays. All the contributions are summarized in Table I.

The uncertainty from luminosity measurement is estimated to be 1.1% using Bhabha events. The muon tracking
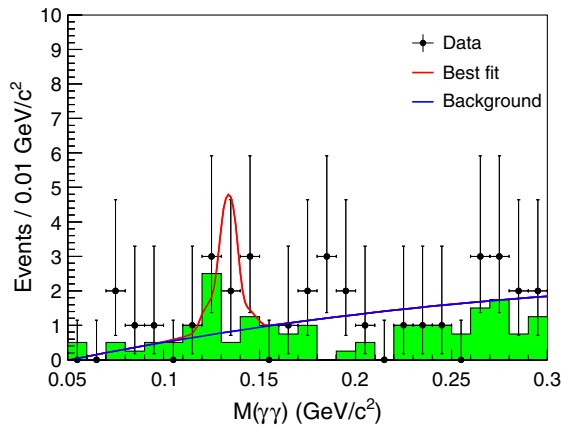
TABLE I. Summary of the systematic errors (%) in the cross section measurement.

Source	$\eta\mu^+\mu^-$	ηe^+e^-	$\pi^0\mu^+\mu^-$
Luminosity	1.1	1.1	1.1
Tracking	2	$\cdots$	2
Photon detection	2	2	2
Lepton resolution	1.6	2.4	1.6
Kinematic fit	1.9	1.9	1.9
Background shape	1.5	3.0	9.4
Fit function	$\cdots$	$\cdots$	3.9
$\psi(4040)$ parameters	2.0	3.3	4.0
Branching fractions	1.2	1.2	1.0
Others	1.0	1.0	1.0
Total	5.0	6.1	11.8

efficiency is estimated to be 1% for each track. Since the luminosity is measured using Bhabha events, the tracking efficiency of electron pairs cancels. The photon detection efficiency is also estimated to be 1% for each photon. The uncertainties associated with the lepton-pair invariant mass resolutions and the kinematic fits are estimated using the $\psi(3686) \to \eta J/\psi$ control sample. It is obtained from the $\psi(3686)$ data sample by imposing the selection criteria described above, and requiring $M(\gamma_H J/\psi) < 3.49$ GeV/c^2 to reject χ_{c1} and χ_{c2} events. This gives a low-background $\psi(3686) \to \eta J/\psi$ events with a purity of 98.5%. The efficiency difference between data and MC simulation for the J/ψ invariant mass window is 1.6% in the $\mu^+\mu^-$ mode and 2.4% in the e^+e^- mode. They are taken as systematic errors due to lepton-pair invariant mass resolution. For the kinematic fit, the efficiency difference between data and MC simulation is 1.9% in both modes.

Uncertainties due to the choice of background shape are estimated by varying the background function from a third-order polynomial to a second-order and a fourth-order polynomial in the fit, and these changes yield a 1.5% difference in $\mu^+\mu^-$ and a 3.0% difference in e^+e^- in the number of η signal events. The $e^+e^- \to \pi^+\pi^-\pi^0$ backgrounds subtraction gives a 9.4% difference in $\mu^+\mu^-$ in the number of π^0 signal events. The uncertainty due to the fit function is estimated by changing the smearing Gaussian parameter by 1 standard deviation in the π^0 signal pdf, which gives 3.9% difference in the number of π^0 signal events. Uncertainties in the $\psi(4040)$ resonance parameters and possible distortions of the $\psi(4040)$ line shape due to interference effects with the nearby $\psi(4160)$ resonance introduce uncertainties in the radiative correction factor and the efficiency. Changing the Breit-Wigner parameters (mass and width) by 1 standard deviation according to PDG values [2] or using a coherent shape with the $\psi(4160)$ resonance [16] results in variations in $(1 + \delta) \times \epsilon$ of 2.0% in $\mu^+\mu^-$ and 3.3% in e^+e^- for the $\eta J/\psi$ measurement and 4.0% in $\mu^+\mu^-$ for $\pi^0 J/\psi$ measurement. The PDG uncertainty in $\mathcal{B}(J/\psi \to \ell^+\ell^-)$ is 1% and $\mathcal{B}(\eta \to \gamma\gamma)$ is 0.5% [2]. Other sources of systematic error, including fake photon simulation and the final-state radiation simulation, are estimated to be 1.0% in total.

Assuming all the sources are independent, the total systematic error on the $\eta J/\psi$ cross section measurement is determined to be 5.0% for $\mu^+\mu^-$ and 6.1% for e^+e^-. Considering the common and uncommon errors for these two modes, the combined systematic error on the $\eta J/\psi$ cross section measurement is 4.0%. The total systematic error is 11.8% in $\mu^+\mu^-$ for the $\pi^0 J/\psi$ cross section measurement by summing up all the errors in quadrature.

Since the significance of the $\pi^0 J/\psi$ signal is low, an upper limit on the $\pi^0 J/\psi$ production cross section is set at $\sigma^B(e^+e^- \to \pi^0 J/\psi) < 1.6$ pb at the 90% confidence level,

where $e^+e^- \to \pi^+\pi^-\pi^0$ backgrounds have been subtracted and the efficiency is lowered by a factor of $(1 - \sigma_{sys})$.

If we assume the observed $\eta J/\psi$ and $\pi^0 J/\psi$ are completely from $\psi(4040)$ decays and use the total cross section of $\psi(4040)$ at $\sqrt{s} = 4.009$ GeV [(6.2 ± 0.6) nb] calculated with the PDG resonance parameters [2] as input, we determine the fractional transition rate $\mathcal{B}(\psi(4040) \to \eta J/\psi) = (5.2 \pm 0.5 \pm 0.2 \pm 0.5) \times 10^{-3}$, where the first, second, and third errors are statistical, systematic, and uncertainty from $\psi(4040)$ resonant parameters, respectively. In addition, we obtain an upper limit on $\mathcal{B}(\psi(4040) \to \pi^0 J/\psi) < 2.8 \times 10^{-4}$ at the 90% confidence level.

In summary, we observe for the first time $e^+e^- \to \eta J/\psi$ production at $\sqrt{s} = 4.009$ GeV with a statistical significance greater than 10σ. The Born cross section is measured to be $(32.1 \pm 2.8 \pm 1.3)$ pb, where the first error is statistical and the second systematic. We do not observe a significant $e^+e^- \to \pi^0 J/\psi$ signal, and the Born cross section is found to be less than 1.6 pb at the 90% confidence level. These measurements do not contradict the upper limits set by the CLEO experiment [9]. The $\eta J/\psi$ cross section measurement is within the range of the theoretical calculation and the $\pi^0 J/\psi$ upper limit does not exclude the prediction [17]. A transition rate of 5×10^{-3} level is measured for $\psi(4040) \to \eta J/\psi$, corresponding to a partial decay width at the 400 keV level, which is much larger than that for $\psi(3770) \to \eta J/\psi$ [8] and is more than 2 times that for $\psi(4040) \to \pi^+\pi^- J/\psi$ [9].

[1] J. Siegrist *et al.*, Phys. Rev. Lett. **36**, 700 (1976).

[2] J. Beringer *et al.* (Particle Data Group), Phys. Rev. D **86**, 010001 (2012).

[3] B. Aubert *et al.* (*BABAR* Collaboration), Phys. Rev. Lett. **95**, 142001 (2005); C. Z. Yuan *et al.* (Belle Collaboration), Phys. Rev. Lett. **99**, 182004 (2007); X. L. Wang *et al.* (Belle Collaboration), Phys. Rev. Lett. **99**, 142002 (2007).

[4] E. Eichten, K. Gottfried, T. Kinoshita, K. Lane, and T. Yan, Phys. Rev. D **17**, 3090 (1978); **21**, 203 (1980); T. Barnes, S. Godfrey, and E. S. Swanson, Phys. Rev. D **72**, 054026 (2005).

[5] For a recent review, see N. Brambilla *et al.*, Eur. Phys. J. C **71**, 1534 (2011).

[6] B. Aubert *et al.* (*BABAR* Collaboration), Phys. Rev. D **78**, 112002 (2008).

[7] M. B. Voloshin, Mod. Phys. Lett. A **26**, 773 (2011).

[8] N. E. Adam *et al.* (CLEO Collaboration), Phys. Rev. Lett. **96**, 082004 (2006).

[9] T. E. Coan *et al.* (CLEO Collaboration), Phys. Rev. Lett. **96**, 162003 (2006).

[10] M. Ablikim *et al.* (BESIII Collaboration), Nucl. Instrum. Methods Phys. Res., Sect. A **614**, 345 (2010).

[11] S. Jadach, B. F. L. Ward, and Z. Was, Comput. Phys. Commun. **130**, 260 (2000); Phys. Rev. D **63**, 113009 (2001).

[12] Ping Rong-Gang, Chinese Phys. C **32**, 599 (2008).

[13] Wang Ping, Ma Yan-Yun, Qin Xiu-Bo, Zhang Zhe, Cao Xing-Zhong, Yu Run-Sheng, and Wang Bao-Yi, Chinese Phys. C **32**, 243 (2008).

[14] http://home.thep.lu.se/~torbjorn/Pythia.html

[15] E. A. Kuraev and V. S. Fadin, Yad. Fiz. **41**, 733 (1985) [Sov. J. Nucl. Phys. **41**, 466 (1985)].

[16] X. L. Wang for the Belle Collaboration, in Proceedings of the FPCP Meeting (unpublished) [http://hepg-work.ustc.edu.cn/fpcp2012].

[17] Q. Wang, G. Li, X. H. Liu, and Q. Zhao, arXiv:1206.4511.